JACS
JOURNAL OF THE AMERICAN CHEMICAL SOCIETY
Article
pubs.acs.org/JACS

Sequence-Selective Detection of Double-Stranded DNA Sequences Using Pyrrole–Imidazole Polyamide Microarrays

Ishwar Singh,[†] Christian Wendeln,[‡] Alasdair W. Clark,[§] Jonathan M. Cooper,[§] Bart Jan Ravoo,*[,‡] and Glenn A. Burley*[,†]

[†]Department of Pure & Applied Chemistry, University of Strathclyde, 295 Cathedral Street, Glasgow G1 1XL, United Kingdom

[‡]Organic Chemistry Institute and Centre for Nanotechnology (CeNTech), Westfälische Wilhelms-Universität Münster, Corrensstrasse 40, 48149 Münster, Germany.

[§]Division of Biomedical Engineering, School of Engineering, University of Glasgow, Oakfield Avenue, Glasgow G12 8LT, United Kingdom

Supporting Information

ABSTRACT: We describe a microarray format that can detect double-stranded DNA sequences with a high degree of sequence selectivity. Cyclooctyne-derivatized pyrrole–imidazole polyamides were immobilized on azide-modified glass substrates using microcontact printing and a strain-promoted azide–alkyne cycloaddition (SPAAC) reaction. These polyamide-immobilized substrates selectively detected a seven-base-pair binding site incorporated within a double-stranded oligodeoxyribonucleotide sequence even in the presence of an excess of a sequence with a single-base-pair mismatch.

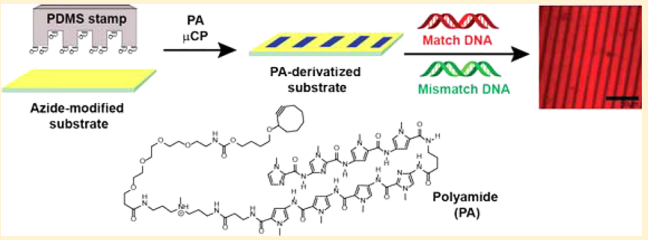

INTRODUCTION

Functionalized microarrays that are capable of recognizing specific biomolecules hold great promise as tools for nanotechnological as well as medical diagnostic applications.[1−4] Compared with traditional low-throughput methods for the analysis of biomolecular binding events such as cell culture assays, microarray technology enables the detection and analysis of the relative abundance and variation of specific biomolecules in a high-throughput screening format.[5,6] DNA microarrays in particular have been widely exploited for the analysis of genotypic variations by detecting the binding of a single-stranded DNA (ssDNA) analyte using complementary ssDNA probes immobilized on a solid substrate.[7,8] The transduction of this binding event into a quantifiable signal such as a change in fluorescence emission can be used to detect as well as quantify the abundance of the corresponding ssDNA analyte.[8,9]

Recent innovations in microarray technology have extended their present capability to include the assessment of recognition profiles of transcription factors[9,10] and small molecules[11−13] in a parallel and high-throughput fashion using double-stranded DNA (dsDNA) probe sequences immobilized on a solid substrate.[11−15] Detection of a dsDNA binding event is achieved either by a reporter directly attached to the DNA-binding molecule[12,13] or via a fluorescently tagged antibody specific for the transcription factor of interest.[9] Both of these microarray formats utilize immobilized dsDNA oligodeoxyribonucleotides (ODNs) to probe the dsDNA binding characteristics of the DNA binder present in solution. To the best of our knowledge, a microarray setup that examines the binding affinity and selectivity of dsDNA-binding molecules where dsDNA is the analyte present in solution has not been reported.

To develop an array setup of this type and assess the scope and limitations of the corresponding format, three developments are required: (i) efficient access to a suite of probe molecules that recognize dsDNA sequences selectively; (ii) the ability of these probe molecules to distinguish a matched dsDNA sequence from mismatched sequences when immobilized on a solid substrate; and (iii) the availability of chemoselective and high-yielding bioconjugation chemistry to immobilize the probe molecules on a substrate in a microarray format. Of the various families of molecules available that bind to dsDNA sequences, we chose pyrrole–imidazole polyamides (PAs) as a paradigm for this study. PAs bind to dsDNA with nanomolar binding affinity in a sequence-selective manner by reading the hydrogen-bonding landscape of the edges of Watson–Crick base pairs (bp) in the minor groove of B-type dsDNA (Figure 1a).[16] They are highly programmable, enabling the identification of dsDNA sequences from 5 to 16 bp in length, thus addressing criteria (i) and (ii) above.[12,13,17]

In this article, we describe a PA microarray format and demonstrate its use for direct and selective detection of dsDNA sequences. The microarray design utilizes microcontact printing (μCP)[18,19] and strain-promoted azide–alkyne cycloaddition (SPAAC)[20,21] to immobilize PA (**1**) onto a glass substrate

Received: September 30, 2012
Published: February 4, 2013

   dx.doi.org/10.1021/ja309677h | J. Am. Chem. Soc. 2013, 135, 3449−3457

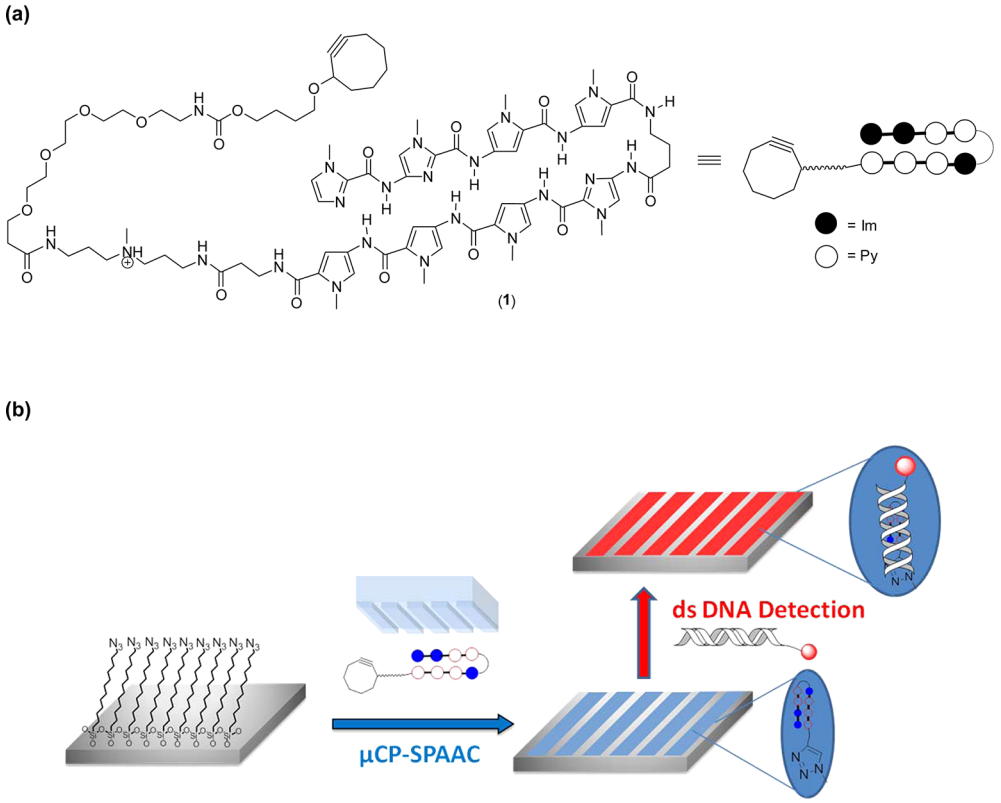

Figure 1. (a) Structure of PA (**1**) used in this study. (b) Schematic depiction of the process of fabricating PA-derivatized surfaces using μCP and SPAAC. A PDMS stamp inked with PA (**1**) is brought into direct contact with an azide-modified surface to produce a PA-patterned surface. The PA-derivatized surface selectively detects fluorophore-tagged ODN duplexes consisting of matched binding sequences.

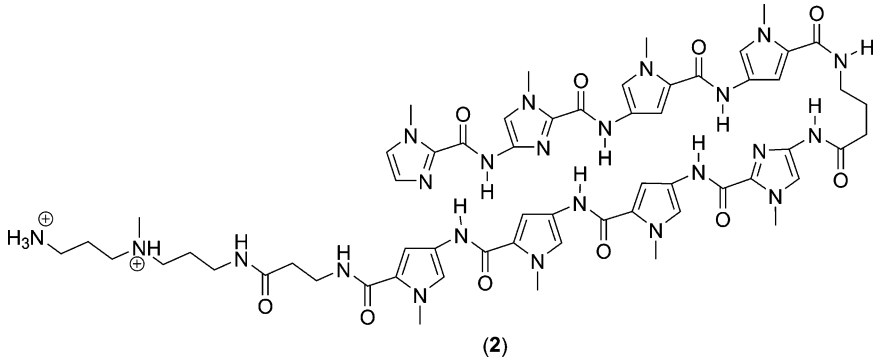

Figure 2. Structure of PA (**2**).

Scheme 1[a]

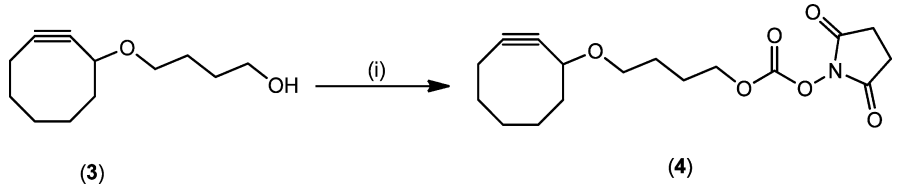

[a]Reagents and conditions: (i) DSC, DIPEA, MeCN, room temperature, 1 h; 76%.

(Figure 1b). Single-base-pair sequence discrimination is observed by the selective detection of fluorescently tagged ODN duplexes containing a 7 bp target binding site matched to the core PA (**2**) (Figure 2), even in the presence of a competing sequence with a single-base-pair mismatch.

EXPERIMENTAL SECTION

Synthesis of 4-(Cyclooct-2-yn-1-yloxy)butyl (2,5-Dioxopyrrolidin-1-yl) Carbonate (4). To a solution of 4-(cyclooct-2-yn-1-yloxy)butan-1-ol (**3**)[22] (70 mg, 0.357 mmol) in acetonitrile (2 mL) was added *N*,*N*′-disuccinimidyl carbonate (DSC) (110 mg, 0.428 mmol) followed by *N*,*N*-diisopropylethylamine (DIPEA) (75 μL,

dx.doi.org/10.1021/ja309677h | J. Am. Chem. Soc. 2013, 135, 3449−3457

Scheme 2[a]

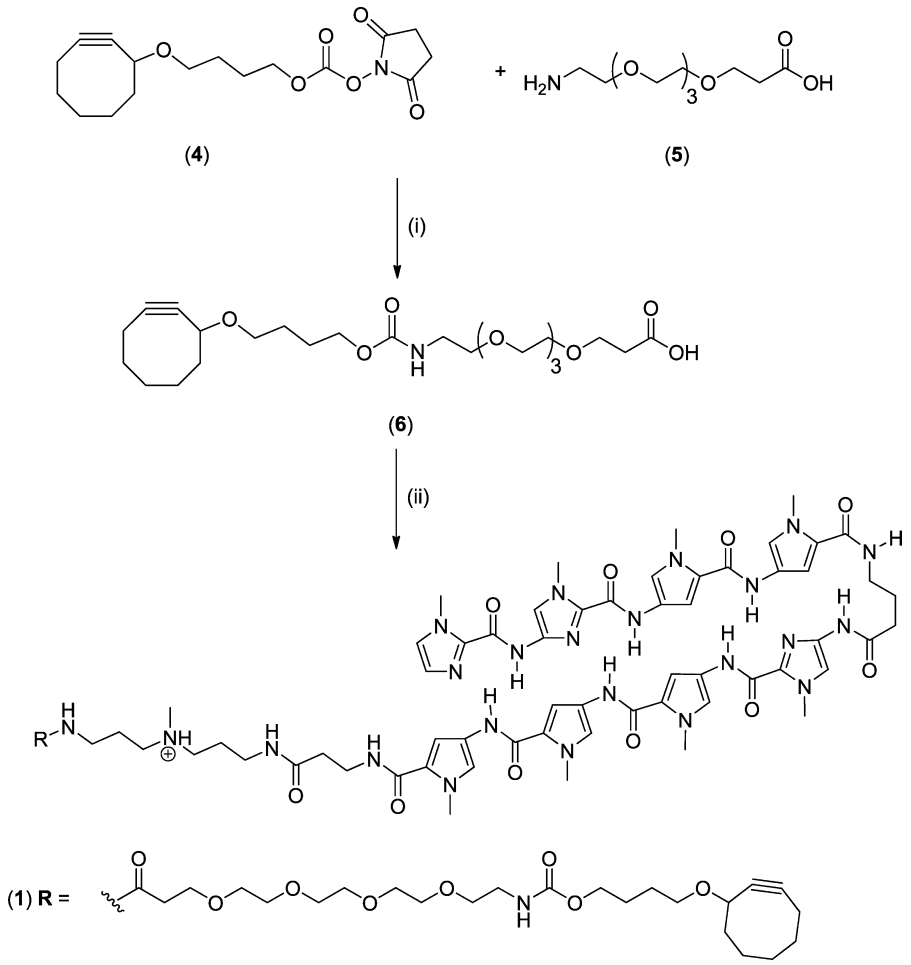

[a]Reagents and conditions: (i) TEA, DCM, room temperature, 20 min; (ii) **2**, HATU, DIPEA, DMF, 1 h; 44% over two steps.

0.428 mmol). The reaction mixture was stirred at room temperature in air for 1 h and then concentrated in vacuo. Column chromatography (SiO_2, gradient from 9:1 to 3:1 hexane/EtOAc) afforded (**4**) (91 mg, 76% yield) as a colorless oil (Scheme 1). ^{1}H NMR (400 MHz, $CDCl_3$): δ 4.38−4.34 (m, 2H), 4.15−4.12 (m, 1H), 3.61−3.55 (m, 1H), 3.37−3.33 (m, 1H), 2.83 (s, 4H), 2.25−2.06 (m, 3H), 1.92−1.81 (m, 6H), 1.70−1.61 (m, 5H). ^{13}C NMR (100 MHz, $CDCl_3$): δ 168.1, 151.0, 99.3, 92.5, 71.9, 70.3, 67.8, 41.8, 33.7, 29.2, 25.8, 25.1, 25.0, 24.9, 20.1. HRMS (ESI+) m/z: calcd for $C_{17}H_{24}O_6N$ $[M + H]^+$, 338.1604; found, 338.1598 (Figure S35 in the Supporting Information).

Synthesis of Polyamide−Cyclooctyne Conjugate (1). To a solution of 15-amino-4,7,10,13-tetraoxapentadecanoic acid (**5**) (3 mg, 0.011 mmol) in 1 mL of dry dichloromethane (DCM) was added a solution of (**4**) (3.8 mg, 0.0113 mmol) in dry DCM (1 mL) followed by triethylamine (TEA) (3 μL, 0.0026 mmol). The reaction mixture was stirred at room temperature for 20 min and then concentrated in vacuo. The crude mixture was redissolved in 1 mL of dry *N*,*N*-dimethylformamide (DMF), and 2-(1*H*-7-azabenzotriazol-1-yl)-1,1,3,3-tetramethyluronium hexafluorophosphate (HATU) (1.8 mg, 0.0047 mmol) and DIPEA (2.8 μL, 0.015 mmol) were added. After the reaction mixture was stirred for 5 min at room temperature, PA (**2**) (2 mg, 0.0015 mmol) was added, and the resulting mixture was stirred for 1 h at room temperature. Purification by semipreparative reversed-phase HPLC (t = 15.1 min) afforded PA (**1**) as a yellow powder after freeze-drying (1.2 mg, 44% yield). For information concerning the buffer system and gradient used in the analysis and purification, see the Supporting Information. HRMS (ESI+) m/z: calcd for $C_{83}H_{115}N_{24}O_{18}$ $[M + H]^+$, 1735.8821; found, 1735.8824 (Figure S37 in the Supporting Information).

Synthesis of *n*-Hexyl Polyamide Cyclooctyne Click Conjugates (7). To a solution of PA (**1**) in dimethyl sulfoxide (DMSO) (75 μL, 0.039 μmol, 533 μM, 1 equiv) was added a solution of *n*-hexyl azide in DMSO (780 μL, 7.8 μmol, 10 mM, 200 equiv). The reaction mixture was shaken at room temperature in air for 24 h. Reversed-phase HPLC revealed the formation of two new peaks (t = 15.7 and 16 min), corresponding to the triazole products (**7a**) and (**7b**) according positive-ion-mode electrospray ionization (ESI+) mass spectrometry (MS). For information concerning the buffer system and gradient used in the HPLC analysis and purification, see the Supporting Information. HRMS (ESI+) m/z: calcd for $C_{89}H_{128}N_{27}O_{18}$ $[M + H]^+$, 1862.9931; found, 1863.0051 (Figure S38 in the Supporting Information).

Preparation of Undecyl Azide-Modified Silicon and Glass Substrates. Undecyl azide-modified substrates were prepared using a modified protocol of a literature procedure.[23] Glass and silicon substrates were cut into small pieces and cleaned by sonication in pentane, acetone, and finally Milli-Q water. The substrates were treated with freshly prepared piranha solution (3:1 H_2SO_4/H_2O_2; **Caution!**) for 30 min. The surfaces were thoroughly washed with Milli-Q water to remove all traces of sulfuric acid and dried under a stream of Ar. The substrates were immersed in a solution of 11-bromoundecyltrichlorosilane (0.1 vol %) in toluene for 40 min and then cleaned by extensive washing with DCM, ethanol, and Milli-Q water. The dry alkyl bromide-functionalized surfaces were converted to azide-functionalized substrates by exposure to a saturated solution of NaN_3 in DMF for 48 h at 70 °C. Finally, the substrates were washed with Milli-Q water and ethanol and dried in a stream of Ar.

dx.doi.org/10.1021/ja309677h | *J. Am. Chem. Soc.* 2013, 135, 3449−3457

Scheme 3[a]

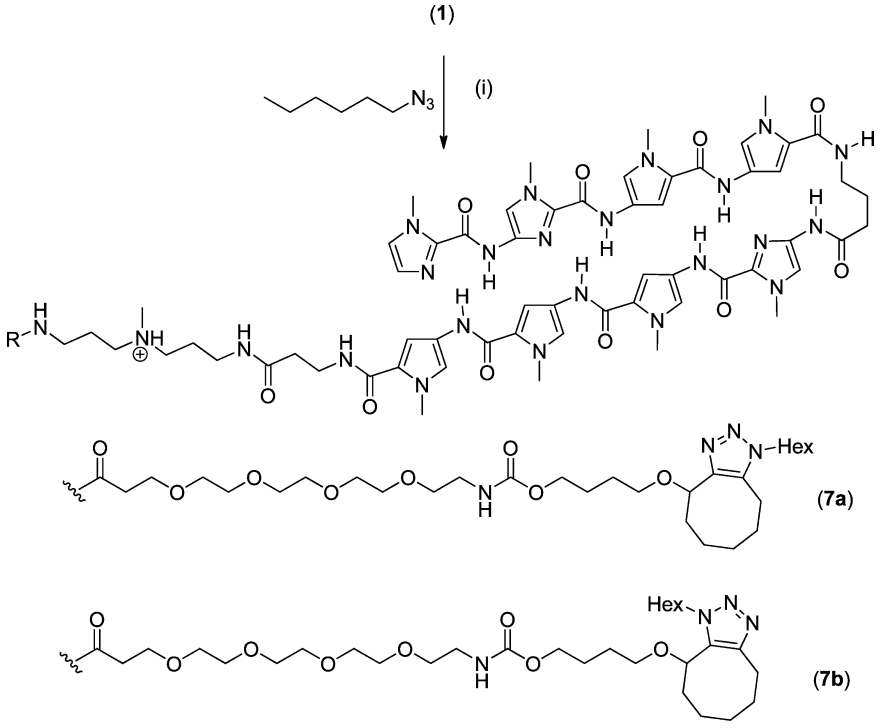

[a]Conditions: (i) DMSO, room temperature, 24 h.

Microcontact Printing. Polydimethylsiloxane (PDMS) stamps (flat, patterned) were oxidized in an UV ozonizer (PSD-UV, Novascan Technologies Inc.) for 55 min directly before use and stored under distilled water. The PDMS stamps were dried in a stream of Ar and subsequently covered with 10−20 μL of a solution of cyclooctyne-modified PA (**1**) in 1:1 methanol/ethanol (concentration ranging from 100 nM to 100 μM). After 1 min, the stamps were blow-dried in a stream of Ar and placed on the undecyl azide-modified substrate surfaces. A weight of 30 g was applied on the top of the PDMS stamps at ambient temperature. After 20−60 min, the PDMS stamps were removed from the surfaces, and the modified substrates were washed with Milli-Q water and ethanol, sonicated in Milli-Q water (1 min), and dried in a stream of Ar (see Figure 3).

dsDNA Binding Protocol Using PA-Derivatized Microarrays. A concentration series of 5′-Cy3-labeled dsDNA (ODN1−4) was prepared [1 μM/500 nM/10 nM/1 nM in 50 mM phosphate buffer (pH 7.5) containing 0.01% Tween 20] and applied to PA-modified glass surfaces. The surfaces were transferred to a moist chamber and stored at room temperature overnight. The unbound dsDNA was removed by washing with 50 mM phosphate buffer (pH 7.5) containing 0.01% Tween 20 for 3 min at room temperature and then for 3 min at 50 °C, after which the washed glass slides were dried under N_2. DNA binding was assessed using confocal fluorescence microscopy.

Competitive dsDNA Binding Assay on the Microarray. Competitive binding assays were performed using a series of mixtures of ODN1 and ODN2 (see Table 3). The binding and washing protocols were performed as described above.

RESULTS AND DISCUSSION

Experimental Design. This work had two principal aims: (i) to develop an efficient and robust synthetic methodology for immobilizing PAs onto solid substrates and (ii) to assess the ability of these PA-derivatized surfaces to bind matched dsDNA sequences selectively. Our design focused on the utility of μCP[24,25] in immobilizing cyclooctyne-modified PA (**1**) onto azide-functionalized glass surfaces (Figure 1).[23] Previous studies showed that DNA microarrays can be prepared easily and cost-effectively by combining μCP with copper-free click chemistry to immobilize DNA strands on glass substrates.[26] In the current work, a SPAAC protocol[20,27−29] was adopted for the immobilization of PA (**1**) ink onto an azide substrate, as it dispels the need for copper(I) catalysis as required in conventional copper-catalyzed Huisgen [3 + 2] azide−alkyne cycloaddition (CuAAC).[30,31] We avoided utilizing CuAAC chemistry because PAs incorporate imidazole units, which have known affinity for copper ions.[32] The core sequence of PA (**1**) was chosen as a paradigm for this study by virtue of its high binding affinity for the target DNA sequence 5′-WWGGWCW-3′ (where W = A/T).[33] A tetraethylene glycol tether was installed between the cyclooctyne unit and the PA core to impart water solubility and endow PA (**1**) with sufficient flexibility to access optimal binding conformations with its corresponding dsDNA target binding site.

Synthesis of PA (1). Amine-terminated PA (**2**) was prepared in 24% yield by solid-phase synthesis of the heterocyclic core using our triphosgene-mediated coupling strategy (Figure 2 and Scheme S1 in the Supporting Information)[34] followed by resin cleavage using 3,3′-diamino-*N*-methyldipropylamine (DMPA). The cyclooctyne linker (**4**) was prepared using *N*,*N*′-disuccinimidyl carbonate (Scheme 1). Coupling of the NHS ester of (**4**) with amino acid (**5**) afforded linker (**6**), which was used directly in the next step without any purification. Finally, compound (**6**) was coupled with PA (**2**) using HATU as the activating agent to obtain PA (**1**) in 44% yield (Scheme 2).

Assessment of the Performance of Strain-Promoted Click Chemistry with PA (1). In the presence of 200 equiv of *n*-hexyl azide, the two triazole regioisomers (**7a**) and (**7b**) were formed from PA (**1**) in quantitative yield in 24 h (Scheme 3), according to HPLC analysis and high-resolution mass

dx.doi.org/10.1021/ja309677h | J. Am. Chem. Soc. 2013, 135, 3449−3457

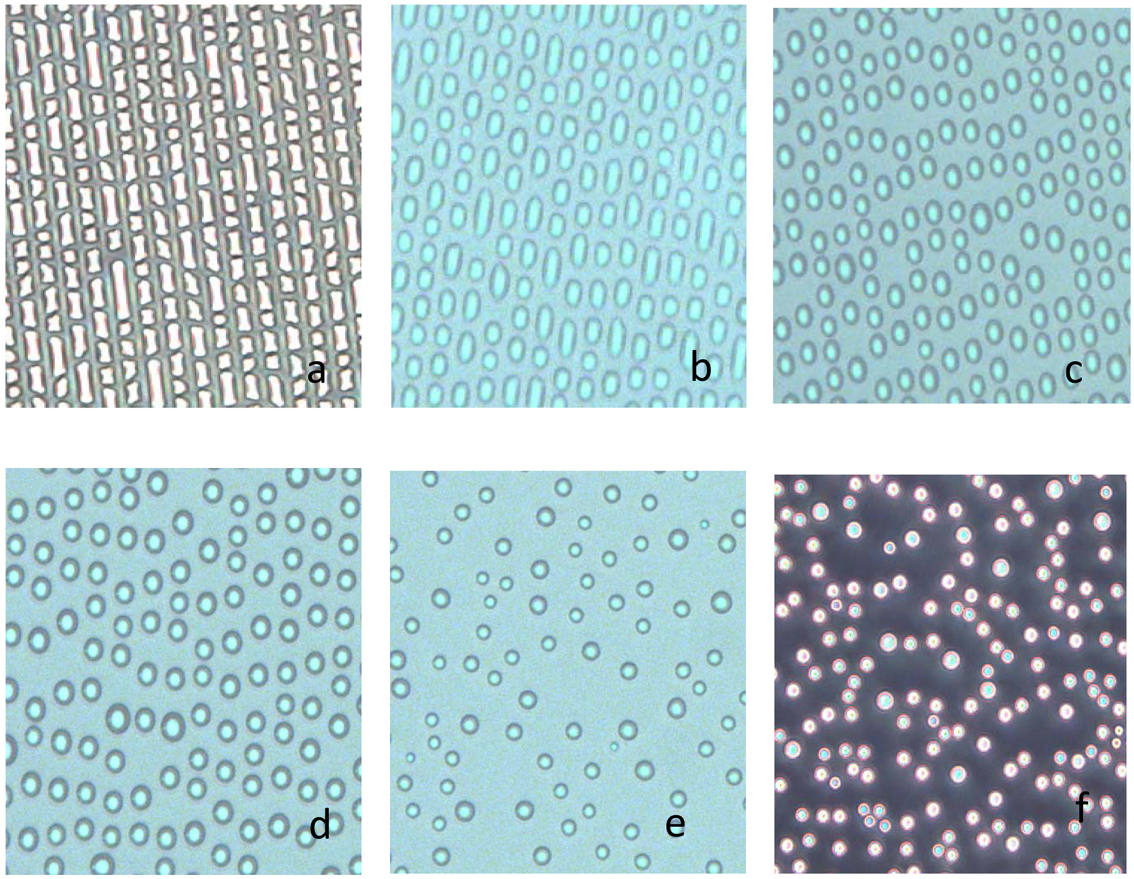

Figure 3. Light microscopy images of water condensation experiments on PA (**1**)-modified glass surfaces: (a) 100 μM PA (**1**), 60 min printing time; (b) 10 μM, 60 min; (c) 1 μM, 60 min; (d) 500 nM, 60 min; (e) 100 nM, 60 min. (f) No pattern was observed when μCP was conducted using an octadecyl-modified glass substrate [100 μM PA (**1**), 10 μm line, and 5 μm space].

Table 1. dsDNA Sequences Used in This Study[a]

ODN1	**Match** (15 mer)	(5`-3`)	CGC-CGA-T**GG-TC**A-TGC
Complementary strand		Cy 3	GCA-TGA-CCA-TCG-GCG
ODN 2	**Mismatch 1**		CGC-CGA-T**G*C*-TC**A-TGC
Complementary strand		Cy 3	GCA-TGA-GCA-TCG-GCG
ODN 3	**Mismatch 2**		CGC-CGA-T**G*T*-*G*C**A-TGC
Complementary strand		Cy 3	GCA-TGC-ACA-TCG-GCG
ODN 4	**Mismatch 3**		CGC-CGA-T***AT*-*G*C**A-TGC
Complementary strand		Cy 3	GCA-TGC-ATA-TCG-GCG

[a]The location of the mismatched sequence is italicized and underlined. The PA target sequence for this study was 5′-WWGGWCW-3′, where W = A/T.

spectrometry (HRMS) (see Figures S33 and S38 in the Supporting Information). This confirmed that the cyclooctyne moiety of PA (**1**) was available to react with a corresponding azide and did not form an unfavorable conformation to sequester its reactivity with the azide surface.

Immobilization of PA (1) on Solid Surfaces by μCP. Oxidized PDMS stamps with a relief structure were inked with a solution of PA (**1**) and brought into contact with undecyl azide-modified substrates. The SPAAC reaction was induced in the area of contact to produce stable, covalent attachment of PA (**1**) on the glass substrate. Because of the more hydrophilic nature of PAs relative to the azide surfaces, immobilization led to a significant decrease in the water contact angle. After μCP of PA (**1**) with a flat stamp (100 μM, 20 min), the advancing contact angle decreased from 82 ± 3° for the undecyl azide monolayer to 62 ± 3° for the PA-modified surface. The receding contact angle decreased even more significantly from 70 ± 3° to 15 ± 5°, providing further evidence of covalent attachment of PAs to the glass surface. Water condensation experiments further confirmed the attachment of PA (**1**), as visualized by the hydrophilic line patterns shown in Figure 3a–e. We observed that the surface density of the immobilized PA residues could be controlled by the concentration of PA (**1**) used for the ink solutions. In the case of concentrated solutions (100 μM), well-defined condensation patterns were obtained, whereas dilute solutions (100 nM) did not cause any visible arrangement of droplets. As a negative control, PA (**1**) was

dx.doi.org/10.1021/ja309677h | J. Am. Chem. Soc. 2013, 135, 3449–3457

Table 2. UV−Vis Melting Temperature Analysis of PA (2) in Complex with ODN1−4

Sequence	Oligonucleotide Sequence (5`- 3`)	DNA only Tm (°C)	DNA + PA	ΔTm (°C)
ODN 1	CGC CGA T**GG TC**A TGC	68.7	77.2 (PA2)	8.5 (Match)
ODN 2	CGC CGA T**GC**TCA TGC	68.1	72.3 (PA2)	4.2 (Mismatch 1)
ODN 3	CGC CGA T**GTG**CA TGC	68.4	70.4 (PA2)	2.0 (Mismatch 2)
ODN 4	CGC CGA T**ATG**CA TGC	65.6	65.8 (PA2)	0.2 (Mismatch 3)

printed (100 μM) on an octadecyl-modified glass substrate. No pattern was observed (Figure 3f).

Further characterization of PA-derivatized surfaces by atomic force microscopy (AFM) and X-ray photoelectron spectroscopy (XPS) was also undertaken. PA-patterned surfaces (5 μm lines spaced by 3 μm) were clearly visible by AFM in height (Figure S1 in the Supporting Information) as well as phase contrast (Figure S2 in the Supporting Information), with the observed height difference of 1.5−2 nm between the azide- and PA-covered surfaces. XPS confirmed the attachment of PA (**1**) to the azide-modified surface. In the case of an undecyl azide monolayer, only saturated C 1s signals (285 eV) and signals for carbons attached to nitrogen (approximately 287 eV) were observed (Figure S3 in the Supporting Information). After μCP of PA (**1**) using a flat stamp, additional shoulders for carbon atoms in a C−O environment (286−287 eV) and in an amide environment (288 eV) were visible, verifying the attachment of PAs to the substrate (Figure S3). Moreover, the absence of the two nitrogen signals in the N 1s region of the undecyl azide monolayer (corresponding to internal and neighboring azide nitrogens) and the presence of a single, broad nitrogen peak for all surface nitrogens (triazole, amide, amine) further corroborated that immobilization of PA (**1**) on the substrate had been achieved (Figure S4 in the Supporting Information).

PA-Derivatized Surfaces Are Selective for Their Target dsDNA Binding Sequence. Table 1 summarizes the dsDNA sequences used to assess the binding affinity and selectivity of PA (**2**) [i.e., the precursor of (**1**)] in solution. The ODN1 duplex contained a matching 7 bp sequence 5′-AT**GGTC**A [the core binding sites of the heterocycles of PA (**2**) are highlighted in bold]. Fluorophore-tagged DNA duplexes containing a 1 bp (ODN2), 2 bp (ODN3), or 3 bp (ODN4) mismatch were also used in this study. UV−vis melting studies of PA (**2**) in complex with ODN1 [i.e., PA(**2**)@ODN1] revealed an 8.5 °C stabilization of the duplex melting temperature (ΔT_m) (Figure S5 in the Supporting Information) relative to free ODN1. In contrast, a stabilization of only 4.2 °C (Figure S6 in the Supporting Information) for PA(**2**)@ODN2 was observed for the 1 bp mismatched ODN2. The stabilizations for the 2 bp (ODN3, ΔT_m = 2.0 °C; Figure S7 in the Supporting Information) and 3 bp (ODN4, ΔT_m = 0.2 °C; Figure S8 in the Supporting Information) mismatched versions were even less pronounced. This study confirmed the selectivity of PA(**2**) to bind to its matched sequence, ODN1 (Table 2).

Assessment of dsDNA Binding to Surfaces Derivatized with PA (1). The ability of the PA-derivatized surfaces to bind target dsDNA sequences selectively was then assessed. Fluorescently tagged Cy3−DNA strands were used as a reporter of a PA−dsDNA binding event. The PA-derivatized surface was incubated in a buffered solution containing ODN1−4 (1 μM and 500 nM) at 23 °C for 12 h. An important aspect in assessing selective binding was washing away excess dsDNA. Initial washing steps of the PA-derivatized surface (three in total) were performed at 23 °C (Figure 5a) in the presence of either the matched ODN1 or the 1 bp mismatched ODN2. An intense fluorescence emission was observed after either excess ODN1 (Figure 4) or ODN2 was washed off, indicating poor sequence discrimination by the immobilized PA surface. In contrast, a 2-fold reduction in the fluorescence intensity of the patterned areas was observed for the 2 bp mismatched duplex ODN3. Finally, no fluorescence emission in the patterned areas was observed in the presence of the 3 bp mismatched ODN4 (Figure 5a). We therefore conclude that our PA-derivatized surface selectively binds to ODN1 (matched) and ODN2 (1 bp mismatch), but discrimination between ODN1 and ODN2 was not possible using washing steps conducted at 23 °C.

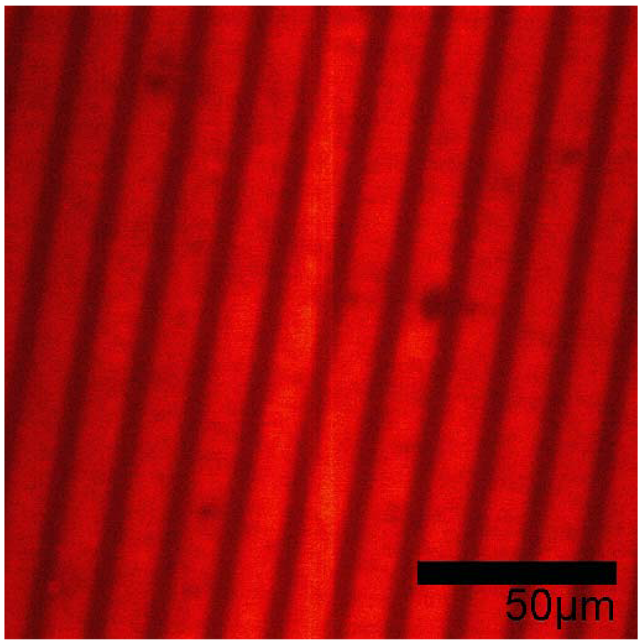

Figure 4. Fluorescence confocal scanning microscopy image of PA-derivatized surfaces (10 μm lines spaced by 5 μm) after incubation with ODN1 (1 μM) and washing (three washing steps in total) at 23 °C.

To improve the sequence selectivity of the process, washing steps (again three in total) were conducted at an elevated temperature of 50 °C. After washing at 50 °C, a 3-fold decrease in the fluorescence emission was observed for the 1 bp mismatched ODN2 relative to the matched ODN1. No fluorescent pattern was visible (i.e., no distinction between the fluorescence emission in the patterned area and the background signal) for either the 2 bp mismatched ODN3 or the 3 bp mismatched ODN4 (Figure 5b). We surmise that enhanced destabilization of the binding of the mismatched sequences (ODN2−4) relative to the matched system (ODN1)

dx.doi.org/10.1021/ja309677h | J. Am. Chem. Soc. 2013, 135, 3449−3457

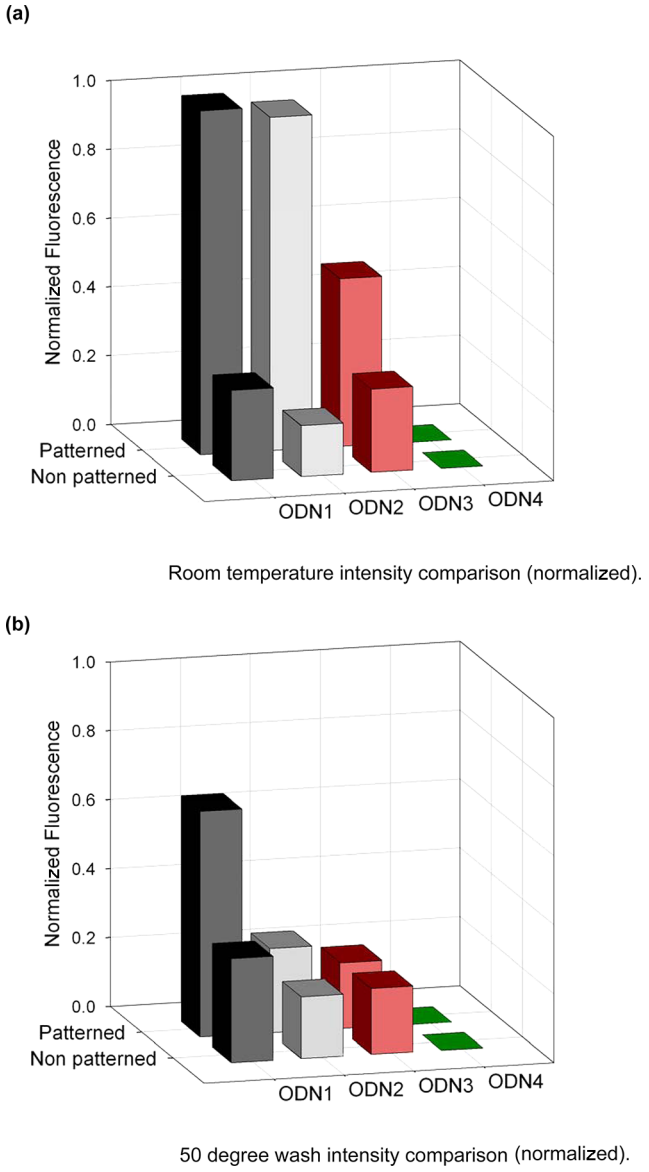

Figure 5. Comparative analysis of the fluorescence intensities of patterned and nonpatterned areas of glass surfaces derivatized with PA (**1**) and exposed to 1 μM concentration of ODN1 (black), ODN2 (gray), ODN3 (red), and ODN4 (green). (a) Washings were conducted in 50 mM phosphate buffer (pH 7.5) containing 0.01% Tween 20 at 23 °C for 3 min. Room temperature intensity comparison (where patterned and nonpatterned areas were indistinct, the same value was used for both; further details of the image analysis can be found in Figures S5 and S9−16 in the Supporting Information). (b) Three washing steps were conducted in 50 mM phosphate buffer (pH 7.5) containing 0.01% Tween 20 at 50 °C for 3 min.

occurs when a washing step is conducted at an elevated temperature.

Competition Assay Using PA-Derivatized Surfaces. The capacity of our PA-derivatized surfaces to detect ODN1 selectively in the presence of 1 bp mismatched ODN2 was then assessed by exposing the surfaces to a series of mixtures of Cy3−ODN1 and ODN2. Within this series, the concentration of Cy3−ODN1 was varied from 500 nM (Table 3, entry 1) down to 50 nM (entry 5) with a commensurate increase in the concentration of ODN2 (i.e., 50 nM in entry 1 to 500 nM in entry 5). Strikingly, very little variation in the fluorescence

Table 3. Competitive Binding Experiments Using PA-Derivatized Substrates[a]

		ODN conc. (nM)		
entry	fluorescence (arb. units)	ODN1	ODN2	ratio
	Cy3−ODN1/ODN2			
1	P: 56.97 ± 6.74	500	50	10:1
	N: 42.8 ± 5.4			
2	P: 51.13 ± 5.8	500	100	5:1
	N: 37.54 ± 5.94			
3	P: 55.55 ± 8.6	500	500	1:1
	N: 39.25 ± 6.09			
4	P: 45.19 ± 5.16	100	500	1:5
	N: 34.26 ± 5.33			
5	P: 49.3 ± 5.46	50	500	1:10
	N: 34.59 ± 5.37			
	ODN1/Cy3−ODN2			
6	no pattern	500	500	1:1

[a]P = patterned area; N = nonpatterned area.

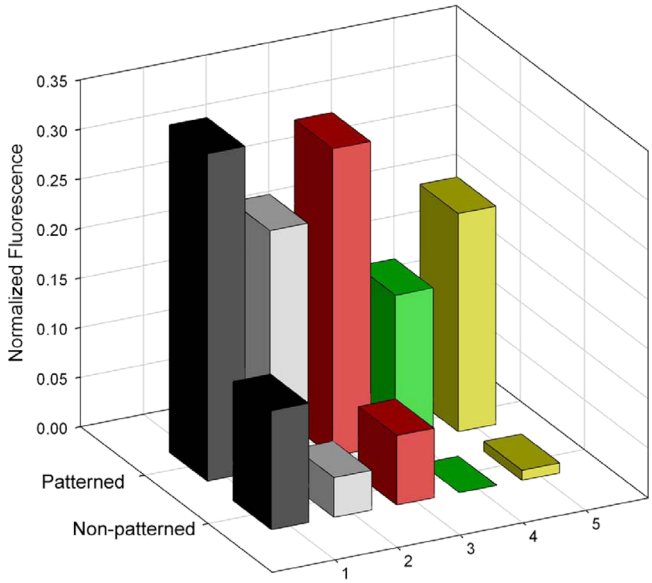

Figure 6. Competitive binding analysis of the fluorescence intensities of patterned and nonpatterned areas of glass surfaces derivatized with PA (**1**) and exposed to Cy3−ODN1/ODN2 mixtures: (1) 500 nM Cy3−ODN1/50 nM ODN2; (2) 500 nM/100 nM; (3) 500 nM/500 nM; (4) 100 nM/500 nM; (5) 50 nM/500 nM. Further details of the image analysis can be found in Figures S21−25 in the Supporting Information.

emission in the presence of increasing amounts of ODN2 was observed in the patterned areas (entries 1−4 and Figure 6), even in the presence of a 10-fold excess of ODN2 (entry 5 and Figure 6). This suggests that the binding preference of PA-derivatized surfaces for ODN1 is not significantly perturbed in the presence of the competing 1 bp mismatched ODN2. The data in entries 1−5 all were obtained with the fluorescence reporter covalently linked to the matched strand. As an additional verification of the results, the fluorescent reporter was transferred to the mismatched ODN2 (Cy3−ODN2; entry 6). A crucial result was the lack of a defined fluorescence pattern observed using an equimolar amount of Cy3−ODN2 and unlabeled ODN1 when this mixture was applied to a PA-printed surface (Figure S26 in the Supporting Information), indicating that the unlabeled matched ODN1 outcompetes

dx.doi.org/10.1021/ja309677h | J. Am. Chem. Soc. 2013, 135, 3449−3457

Cy3−ODN2 for the PA-binding sites on the surface. We therefore conclude that our PA-derivatized surface is selective for ODN1 even in the presence of an excess of the competing mismatched sequence ODN2.

Nanomolar Detection of Matched dsDNA Sequences Using PA-Derivatized Surfaces. Finally, the limit of detection of our PA-derivatized microarray exemplar was then assessed as a function of the concentration of ODN1−4 (concentration series ranging from 1 μM to 1 nM) using our optimized binding and washing protocol. A distinct difference in the fluorescence emissions of the patterned and non-patterned areas was observed using ODN1 down to 10 nM (Figure S27 in the Supporting Information). No fluorescence emission pattern was observed at this concentration in case of the 1 bp mismatched ODN2. Furthermore, no pattern was visible (i.e., no distinction between the fluorescence emission and the background signal could be observed) when PA-derivatized surfaces were exposed to 2 bp mismatched ODN3 or 3 bp mismatched ODN4 at 10 nM, thus confirming that PAs can detect dsDNA sequences selectively when immobilized on solid substrates.

■ DISCUSSION

This study was designed to test whether PAs maintained their ability to bind to their target dsDNA binding sequence selectively when immobilized on a flat surface. We discuss here several conclusions that emerged from our results.

The Temperature of the Washing Step Enhances the Sequence Selectivity of the PA-Derivatized Microarray. Discrimination between the matched sequence (ODN1) and the 1 bp mismatched sequence (ODN2) was observed when a washing procedure was applied at an elevated temperature, in this case 50 °C. The application of a washing step conducted at an elevated temperature is a well-established method for suppressing mismatched binding in DNA microarrays.[35,36] The ionic strength of the buffer is another possible parameter that can be tuned to enhance the discrimination between matched and mismatched binding regimes in DNA microarrays.[35−38] In this study, only the temperature variable was investigated, but there is significant scope to optimize the selectivity of dsDNA binding using PA-derivatized arrays by investigating variation of both the temperature and the ionic strength in future testing cascades. Recent innovations in engineered microfluidic devices, for example, have been developed for DNA microarrays and could be adapted to investigate their utility in optimizing selective dsDNA binding with PA-derivatized microarrays.[35,36]

An unexpected result was the high degree of sequence selectivity for the matched sequence (Cy3−ODN1) even in the presence of an excess of the mismatched one (ODN2). The fluorescence emission observed from the PA microarray was effectively the same whether the concentration of Cy3−ODN1 was 500 nM (Table 3, entry 1) or 50 nM (entry 5). We rationalize this result as follows: At 50 nM Cy3−ODN1, all of the PA-binding sites on the substrate were saturated. Thus, the use of more concentrated samples of Cy3−ODN1 (e.g., entries 1−4) did not result in a further enhancement of the fluorescence emission in the patterned areas. When the fluorophore was transferred from ODN1 to the mismatched sequence (Cy3−ODN2; entry 6), the PAs present on the surface were saturated with nonfluorescent ODN1, and as a result, no defined fluorescence pattern was observed in the PA-patterned areas. Therefore, we can conclude that the matched sequence ODN1 can outcompete the challenging 1 bp mismatched competitor ODN2 in this 50−500 nM regime using our PA-derivatized surfaces.

PAs Maintain Their dsDNA Sequence Selectivity When Immobilized on a Solid Substrate. A significant outcome arising from this study is the ability of PAs to retain their sequence selectivity when bound to a flat surface. PAs tethered to gold nanoparticles, for example, exhibit excellent mismatch discrimination of dsDNA duplexes using a gold aggregation assay.[39] This study has shown that this phenomenon can be extended to a microarray format using μCP as the fabrication method. We predict that further optimization of the selectivity and sensitivity of these arrays could be achieved by (i) optimizing the temperature and washing steps and (ii) changing the reporter module from fluorescence emission to a more sensitive technique such as surface-enhanced resonance Raman spectroscopy.[39,40]

■ CONCLUSIONS

We have demonstrated for the first time a new microarray format that can detect dsDNA sequences with nanomolar sensitivity and very good mismatch discrimination. Since PAs have demonstrated binding affinity and selectivity for sequences up to 16 bp in length,[17] the development of PA-based microarrays targeting unique dsDNA genomic sequences (i.e., >12 bp) is indeed a possibility. Since microarray technology offers superior throughput capabilities and is generally less expensive than other methods such as next-generation sequencing,[41,42] the development of a binding platform of this type could offer an initial high-throughput screening tool to interrogate the dsDNA binding profile of small-molecule ligands that could be used upstream of a more detailed but lower-throughput technique such as deep sequencing.[43−45]

A second and potentially powerful application of this technology could be its utility in structural DNA nanotechnology. PAs are effective ligands for programming the assembly of functional materials along DNA duplexes[46] and nanostructures.[47,48] Our proposed technology could therefore offer the DNA nanotechnology field new opportunities to facilitate the immobilization of DNA nanostructures in predefined locations, for example.[47−50] Future developments will now focus on optimizing the sensitivity, sequence selectivity, and throughput as well as developing these methods into a more generalized label-free platform for the analysis of PA binding for both biological and nanotechnological applications.

■ ASSOCIATED CONTENT

Supporting Information

Synthesis and characterization of PAs, characterization of PA-derivatized substrates, and fluorescence analysis of DNA-binding to PA-derivatized surfaces. This material is available free of charge via the Internet at http://pubs.acs.org.

■ AUTHOR INFORMATION

Corresponding Author

b.j.ravoo@uni-muenster.de; glenn.burley@strath.ac.uk

Notes

The authors declare no competing financial interest.

■ ACKNOWLEDGMENTS

G.A.B. acknowledges the EPSRC for financial support via an Advanced Research Fellowship (EP/E055095/1) and a Follow-on-Fund Grant (EP/H02915X/1). B.J.R. thanks the DFG (Ra1732/2) for financial support.

■ REFERENCES

(1) Yoo, S. M.; Choi, J. H.; Lee, S. Y.; Yoo, N. C. *J. Microbiol. Biotechnol.* **2009**, *19*, 635.
(2) Sassolas, A.; Leca-Bouvier, B. D.; Blum, L. J. *Chem. Rev.* **2008**, *108*, 109.
(3) Carter, N. P. *Nat. Genet.* **2007**, *39*, S16.
(4) Gilad, Y.; Borevitz, J. *Curr. Opin. Genet. Dev.* **2006**, *16*, 553.
(5) Syvanen, A. C. *Nat. Rev. Genet.* **2001**, *2*, 930.
(6) Ghosh, I.; Stains, C. I.; Ooi, A. T.; Segal, D. J. *Mol. BioSyst.* **2006**, *2*, 551.
(7) Howell, A.; Sims, A. H.; Ong, K. R.; Harvie, M. N.; Evans, D. G. R.; Clarke, R. B. *Nat. Clin. Pract. Oncol.* **2005**, *2*, 635.
(8) Hoheisel, J. D. *Nat. Rev. Genet.* **2006**, *7*, 200.
(9) Berger, M. F.; Philippakis, A. A.; Qureshi, A. M.; He, F. S.; Estep, P. W., III; Bulyk, M. L. *Nat. Biotechnol.* **2006**, *24*, 1429.
(10) Stormo, G. D.; Zhao, Y. *Nat. Rev. Genet.* **2010**, *11*, 751.
(11) Carlson, C. D.; Warren, C. L.; Hauschild, K. E.; Ozers, M. S.; Qadir, N.; Bhimsaria, D.; Lee, Y.; Cerrina, F.; Ansari, A. Z. *Proc. Natl. Acad. Sci. U.S.A.* **2010**, *107*, 4544.
(12) Warren, C. L.; Kratochvil, N. C. S.; Hauschild, K. E.; Foister, S.; Brezinski, M. L.; Dervan, P. B.; Phillips, G. N.; Ansari, A. Z. *Proc. Natl. Acad. Sci. U.S.A.* **2006**, *103*, 867.
(13) Puckett, J. W.; Muzikar, K. A.; Tietjen, J.; Warren, C. L.; Ansari, A. Z.; Dervan, P. B. *J. Am. Chem. Soc.* **2007**, *129*, 12310.
(14) Tse, W. C.; Boger, D. L. *Acc. Chem. Res.* **2004**, *37*, 61.
(15) Tse, W. C.; Boger, D. L. *Chem. Biol.* **2004**, *11*, 1607.
(16) Dervan, P. B.; Edelson, B. S. *Curr. Opin. Struct. Biol.* **2003**, *13*, 284.
(17) Trauger, J. W.; Baird, E. E.; Dervan, P. B. *J. Am. Chem. Soc.* **1998**, *120*, 3534.
(18) Wendeln, C.; Singh, I.; Rinnen, S.; Schulz, C.; Arlinghaus, H. F.; Burley, G. A.; Ravoo, B. J. *Chem. Sci.* **2012**, *3*, 2479.
(19) Wendeln, C.; Ravoo, B. J. *Langmuir* **2012**, *28*, 5527.
(20) Jewett, J. C.; Bertozzi, C. R. *Chem. Soc. Rev.* **2010**, *39*, 1272.
(21) Sletten, E. M.; Bertozzi, C. R. *Angew. Chem., Int. Ed.* **2009**, *48*, 6974.
(22) Singh, I.; Heaney, F. *Chem. Commun.* **2011**, *47*, 2706.
(23) Balachander, N.; Sukenik, C. N. *Langmuir* **1990**, *6*, 1621.
(24) Mehlich, J.; Ravoo, B. J. *Org. Biomol. Chem.* **2011**, *9*, 4108.
(25) Ravoo, B. J. *J. Mater. Chem.* **2009**, *19*, 8902.
(26) Rozkiewicz, D. I.; Gierlich, J.; Burley, G. A.; Gutsmiedl, K.; Carell, T.; Ravoo, B. J.; Reinhoudt, D. N. *ChemBioChem* **2007**, *8*, 1997.
(27) Singh, I.; Freeman, C.; Madder, A.; Vyle, J. S.; Heaney, F. *Org. Biomol. Chem.* **2012**, *10*, 6633.
(28) Singh, I.; Freeman, C.; Heaney, F. *Eur. J. Org. Chem.* **2011**, 6739.
(29) Singh, I.; Vyle, J. S.; Heaney, F. *Chem. Commun.* **2009**, 3276.
(30) Tornoe, C. W.; Christensen, C.; Meldal, M. *J. Org. Chem.* **2002**, *67*, 3057.
(31) Kolb, H. C.; Finn, M. G.; Sharpless, K. B. *Angew. Chem., Int. Ed.* **2001**, *40*, 2005.
(32) Birker, P. J. M. W. L.; Hendriks, H. M. J.; Reedijk, J.; Verschoor, G. C. *Inorg. Chem.* **1981**, *20*, 2408.
(33) White, S.; Szewczyk, J. W.; Turner, J. M.; Baird, E. E.; Dervan, P. B. *Nature* **1998**, *391*, 468.
(34) Su, W.; Gray, S. J.; Dondi, R.; Burley, G. A. *Org. Lett.* **2009**, *11*, 3910.
(35) Petersen, J.; Poulsen, L.; Birgens, H.; Dufva, M. *PLoS One* **2009**, *4*, No. e4808.
(36) Petersen, J.; Poulsen, L.; Petronis, S.; Birgens, H.; Dufva, M. *Nucleic Acids Res.* **2008**, *36*, No. e10.
(37) Pozhitkov, A. E.; Stedtfeld, R. D.; Hashsham, S. A.; Noble, P. A. *Nucleic Acids Res.* **2007**, *35*, No. e70.
(38) Binder, H.; Krohn, K.; Burden, C. J. *BMC Bioinf.* **2010**, *11*, 291.
(39) Krpetić, Ž.; Singh, I.; Su, W.; Guerrini, L.; Faulds, K.; Burley, G. A.; Graham, D. *J. Am. Chem. Soc.* **2012**, *134*, 8356.
(40) Guerrini, L.; Graham, D. *Chem. Soc. Rev.* **2012**, *41*, 7085.
(41) Roh, S. W.; Abell, G. C. J.; Kim, K.-H.; Nam, Y.-D.; Bae, J.-W. *Trends Biotechnol.* **2010**, *28*, 291.
(42) Hurd, P. J.; Nelson, C. J. *Briefings Funct. Genomics Proteomics* **2009**, *8*, 174.
(43) Bock, C. *Nat. Rev. Genet.* **2012**, *13*, 705.
(44) Minoshima, M.; Bando, T.; Sasaki, S.; Fujimoto, J.; Sugiyama, H. *Nucleic Acids Res.* **2008**, *36*, 2889.
(45) Meier, J. L.; Yu, A. S.; Korf, I.; Segal, D. J.; Dervan, P. B. *J. Am. Chem. Soc.* **2012**, *134*, 17814.
(46) Su, W.; Schuster, M.; Bagshaw, C. R.; Rant, U.; Burley, G. A. *Angew. Chem., Int. Ed.* **2011**, *50*, 2712.
(47) Cohen, J. D.; Sadowski, J. P.; Dervan, P. B. *J. Am. Chem. Soc.* **2008**, *130*, 402.
(48) Cohen, J. D.; Sadowski, J. P.; Dervan, P. B. *Angew. Chem., Int. Ed.* **2007**, *46*, 7956.
(49) Pinheiro, A. V.; Han, D.; Shih, W. M.; Yan, H. *Nat. Nanotechnol.* **2011**, *6*, 763.
(50) Kershner, R. J.; Bozano, L. D.; Micheel, C. M.; Hung, A. M.; Fornof, A. R.; Cha, J. N.; Rettner, C. T.; Bersani, M.; Frommer, J.; Rothemund, P. W. K.; Wallraff, G. M. *Nat. Nanotechnol.* **2009**, *4*, 557.

■ NOTE ADDED AFTER ASAP PUBLICATION

The version of this article posted ASAP on February 21, 2013, contained errors in Schemes 2 and 3. The corrected version was reposted on February 22, 2013.